ELSEVIER

Contents lists available at ScienceDirect

Applied Geochemistry

journal homepage: www.elsevier.com/locate/apgeochem



Bioremediation of arsenic-contaminated groundwater by sequestration of arsenic in biogenic pyrite



James A. Saunders*, Ming-Kuo Lee**, Prakash Dhakal¹, Shahrzad Saffari Ghandehari, Ted Wilson, M. Zeki Billor, Ashraf Uddin

Department of Geosciences, 2050 Beard-Eaves Memorial Coliseum, Auburn University, Auburn, AL, 36849, USA

ARTICLE INFO

Editorial handling by Dr T Pichler Keywords: Arsenic Sulfate reducing bacteria Bioremediation Arsenian pyrite

ABSTRACT

Pyrite (FeS2) is the most common sulfide mineral in the Earth's crust, and it commonly contains minor amounts of arsenic. Here we show that authigenic pyrite can remove arsenic from contaminated groundwater and this can be used as a new and relatively inexpensive remediation process. Laboratory batch experiments presented show that fine-grain natural pyrite is an effective sorber of dissolved arsenic. Arsenic sorption onto pyrite is shown to increase with increasing pH, particularly at pH > 5 and at elevated dissolved arsenic concentration. We also present results from a field experiment at an arsenic-contaminated industrial site, which demonstrates the results of stimulation of natural sulfate-reducing bacteria in groundwater by injection of a labile organic carbon source, iron, and sulfate. Within a week, bacterial sulfate reduction triggered the formation of biogenic pyrite nanoparticles, which sequestered arsenic by adsorption and co-precipitation. Microscopic and X-ray diffraction analyses confirmed that pyrite was the only iron-sulfide formed, and that no arsenic-only sulfide phase precipitated (e.g. orpiment or realgar). Pyrite occurs as either 1-10 µm euhedral crystals or similar-sized framboids both of which contain 500-4000 mg/kg arsenic. As a result, dissolved arsenic decreased from its initial concentration of 0.3-0.5 mg/L to below the regulatory clean-up standard for the site of 0.05 mg/L in a matter of weeks. In addition to the potential of this technique to remediate anthropogenic arsenic contamination, it is possible that it can be modified to inexpensively treat individual small drinking-water wells contaminated by natural sources of arsenic in many developing nations.

1. Introduction

The concept of stimulating sulfate-reducing bacteria (SRB) to produce biogenic pyrite as a potential groundwater remediation approach for arsenic and metals was first proposed by Saunders et al. (1996), based on research that showed that arsenic and other trace elements were common in recent marine sediments (Huerta-Diaz and Morse, 1992) and also in terrestrial systems, such as in Holocene stream floodplain deposits (Saunders et al., 1997). This proposed approach was evaluated in laboratory experiments by Keimowitz et al. (2005, 2007). Keimowitz et al. (2007) also proposed that a technology based on stimulating SRB metabolism might prove useful in bioremediating groundwater contaminated by arsenic, similar to the approach of Saunders et al. (2005a), who demonstrated in a field study that indigenous SRB could be stimulated to bioremediate lead, zinc, and cadmium in contaminated groundwater. Kirk et al. (2004) observed

that where natural SRB activity occurs in groundwater aquifer systems, low concentrations of arsenic are typically observed. Wolthers et al. (2005a) tracked iron-sulfide formation and its effect on dissolved arsenic in laboratory experiments, and showed that arsenian pyrite efficiently sequesters arsenic from solution. Saunders et al. (2008) reported on reconnaissance experiments designed to stimulate biogenic sulfate reduction in a shallow "tube" well installed in a naturally arseniccontaminated aquifer in Bangladesh, and showed that SRB metabolism lowered groundwater arsenic concentrations. A number of recent laboratory experiments were conducted to evaluate the effects of anaerobic bacterial sulfate reduction and subsequent iron-sulfide biomineralization on dissolved arsenic (Kirk et al., 2010; Onstott et al., 2011; Omoregie et al., 2013; and Sun et al., 2016). In addition, a laboratory investigation by Xie et al. (2016) showed that inorganically formed pyrite, which coated quartz grains during their experiments, was effective in removing As(III) for solution. Finally, Pi et al. (2017)

^{*} Corresponding author.

^{**} Corresponding author.

E-mail addresses: saundja@auburn.edu (J.A. Saunders), leeming@auburn.edu (M.-K. Lee).

¹ Present address: Soil, Water, and Environmental Sciences, University of Arizona, Tucson, AZ, 85719, USA.

J.A. Saunders et al. Applied Geochemistry 96 (2018) 233–243

conducted a short ($\sim\!1$ month-long) field demonstration of stimulating SRB to remove arsenic from groundwater.

Arsenic sorption onto natural and synthetic pyrite has been examined by some researchers (Zouboulis et al., 1993; Han and Fyfe, 2000; Farquhar et al., 2002; Kim and Bachelor, 2009; Han et al., 2013; Bulut et al., 2014) and all the previous research has shown pyrite to be an effective sorber of dissolved arsenic. As a result, Zouboulis et al. (1993), Han and Fyfe (2000), and Bulut et al. (2014) have all proposed that pyrite could prove useful in treating arsenic-contaminated waste waters (e.g. as an above-ground engineering process). The previous research has typically focused on the use of synthetic pyrite to sorb arsenic, with the exception of Bulut et al. (2014). Here we investigate the sorptive capacity of natural pyrite of varying grain sizes and over a wider range of pH than was investigated by Bulut et al. (2014). Our intent is to use these experimental results as a very conservative assessment of the capacity of natural pyrite surfaces to sorb arsenic, which we interpret below as the first step in the incorporation of arsenic into the growing pyrite crystals that form during bioremediation.

Here we present some of the initial results of an ongoing, long-term field demonstration of groundwater arsenic bioremediation. The process has been specifically designed to stimulate SRB to make biogenic pyrite, which removes arsenic from contaminated groundwater at an industrial site in northern Florida, USA. For this paper, we focus on the geochemistry and mineralogy of iron sulfides produced in the experiment, and the efficacy of using pyrite to remove arsenic from groundwater, similar to the approach that was demonstrated for lead, zinc, and cadmium removal (Lee and Saunders, 2003; Saunders et al., 2005a, 2008).

1.1. Arsenic geochemistry and mineralogy

The general geochemistry and mineralogy of arsenic has been discussed in detail previously (e.g., Smedley and Kinniburgh, 2002; Nordstrom and Archer, 2003; O'Day et al., 2004; Ford et al., 2007; Saunders et al., 2008; and Bowell et al., 2014), and thus we present only a brief summary here. Common arsenic minerals include scorodite (FeAsO₄•2H₂O), which forms under oxidizing conditions, and realgar (AsS), orpiment (As₂S₃), and arsenopyrite (FeAsS) that form under reducing conditions. Aqueous arsenic occurs in two oxidation states, As (V) (arsenate) and As(III) (arsenite) and the distribution of the important species are shown in Fig. 1 in Eh-pH space for the As-S-H₂O system. In iron-deficient systems, and taking into account thermodynamic data for thioarsenite complexes (e.g. Wilkin et al., 2003), the restricted stability fields for orpiment and realgar are shown in Fig. 1. Addition of iron to the system leads to displacement of the stability fields of orpiment and realgar by either arsenopyrite (e.g. Langner et al., 2013, Supporting information) or arsenian pyrite (Saunders et al., 2008). Orpiment, realgar, and arsenopyrite are typically formed under hydrothermal conditions and can be associated with more valuable minerals in ores, and thus can be important mineral phases (and sources of arsenic) found in some mine tailings. Realgar and "amorphous" orpiment (Le Pape et al., 2017) and arsenopyrite (Rittle et al., 1995; Onstott et al., 2011) have reportedly been synthesized in low-temperature laboratory experiments utilizing SRB consortia, although only realgar has been confirmed by XRD. Secondary (authigenic) realgar has been reported (with no XRD confirmation) from mine tailings (Walker et al., 2009; DeSisto et al., 2016), in an anthropogenically arseniccontaminated shallow aquifer (O'Day et al., 2004), and in lignite (Langner et al., 2012, 2013). Langner et al. (2013) also report arsenopyrite in lignite (also with no XRD confirmation). Crystalline and/or amorphous realgar and orpiment have also been reported from cooled hydrothermal discharges (e.g., Webster, 1990; Godelitsas et al., 2015). However, based on a number of investigations, it is apparent that under most natural reducing groundwater conditions (pH in range of 5-8) that arsenian pyrite is the most important mineral host for arsenic (Saunders et al., 1996, 2008, 1997; Price and Pichler, 2006; Lowers et al., 2007;

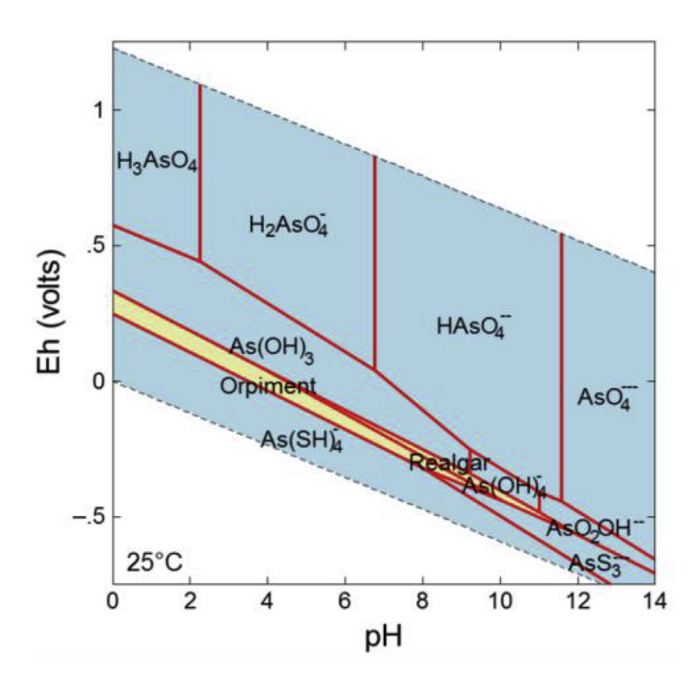


Fig. 1. Eh-pH diagram calculated for As-S-H $_2$ O system at 25 °C and fixed arsenic and sulfate activities of 10^{-6} and 10^{-5} , respectively. The results show the stability field of different arsenic species under different geochemical conditions. Plot was constructed using Geochemist's Workbench including thermodynamic data listed in the Appendix.

Mango and Ryan, 2015; Pi et al., 2016; Houben et al., 2017). Further, arsenian pyrite is common in recent marine and lacustrine sediments as well (Huerta-Diaz and Morse, 1992; Neumann et al., 2013), in recent peat deposits (Langner et al., 2012; Stuckey et al., 2015), and also in coal seams (Kolker et al., 2001).

Aqueous systems containing dissolved sulfide species, which are necessary to form iron (arsenic)-sulfide minerals, also form stable aqueous thioarsenite complexes that can significantly enhance arsenic mobility under reducing conditions (Wilkin et al., 2003; Bostick et al., 2005). However, these thioarsenite aqueous complexes become less important if iron is present in the system, as it removes aqueous sulfide species by forming solid iron sulfide phases (Wilkin et al., 2003; Burton et al., 2014). Finally, another important control on aqueous arsenic geochemistry is the sorption of arsenic onto common aquifer minerals such as iron oxides and oxyhydroxides (e.g. Farquhar et al., 2002; Dixit and Hering, 2003; Giménez et al., 2007) and iron sulfides (Farquhar et al., 2002; Bostick and Fendorf, 2003; Wolthers et al., 2005b; Han et al., 2013; Bulut et al., 2014; this study). The stability of minerals (oxide or sulfide) capable of sorbing arsenic has important implications for arsenic release to the hydrosphere. For example, the reductive dissolution of iron oxyhydroxides that had previously sorbed arsenic by Fe (III)-reducing anaerobic bacteria, is apparently the major cause of natural arsenic contamination of groundwater in Holocene aquifers of SE Asia and elsewhere (Nickson et al., 2000, 2005; McArthur et al., 2004; Saunders et al., 2005c; Fendorf et al., 2010). Conversely, oxidation of arsenic-bearing pyrite in aquifers is also a major source of groundwater contamination (Smedley and Kinniburgh, 2002; Price and Pichler, 2006; Bowell et al., 2014; Mango and Ryan, 2015; Houben et al., 2017). The fact that pyrite can be both a sink and a source for arsenic in groundwater system has led to some confusion about the in environmental geochemistry or arsenic (Saunders et al., 2008).

1.2. Pyrite and arsenian pyrite occurrence and geochemistry

Pyrite is by far the most common iron sulfide phase formed in nature and definitely the most commonly preserved iron sulfide phase in the geologic record (Rickard and Luther, 2007). Other less-common

J.A. Saunders et al. Applied Geochemistry 96 (2018) 233–243

iron sulfide phases can form at low temperature, such as mackinawite (FeS), greigite (Fe₃S₄), and marcasite (FeS₂) (Schoonen and Barnes, 1991; Schoonen, 2004). Rarely, monoclinic pyrrhotite (Fe_{1-x}S) can also form at low temperature due to biogenic sulfate reduction (Saunders and Swann, 1994; Rickard and Luther, 2007). A significant amount of research has shown that pyrite most easily forms at low temperatures by inversion from crystalline or amorphous iron monosulfide precursors (e.g. mackinawite), but the exact mechanism and the importance of this pathway is debated (see summaries and references in Benning et al., 2000; Schoonen, 2004; Rickard and Luther, 1997). Given the rapid formation of pyrite in this study (see below), we conclude that either pyrite directly precipitated from the amended groundwater during the early stages of bioremediation, or that it inverted from an iron monosulfide precursor in a matter of a few days. The exact mechanisms of arsenic-sequestration capabilities of pyrite demonstrated in this study require further study, but the formation of arsenian pyrite apparently is capable of removing dissolved arsenic effectively. However, one study showed that iron sulfide precursor inversion to pyrite can be retarded by the presence of dissolved arsenic (Wolthers et al., 2007).

Pyrite can contain up to 10 wt.% arsenic (Abraitis et al., 2004), but there is also uncertainty about the exact method of incorporation of arsenic into iron sulfides. Studies have shown that mackinawite can sorb arsenic efficiently (Farquhar et al., 2002; Wolthers et al., 2005b; Burton et al., 2014), but if mackinawite formed in natural systems and sorbed arsenic from solution, it is not clear what the fate of the sorbed arsenic would be if the mackinawite inverts to pyrite. It is clear from recent research that arsenic also can be effectively sorbed by pyrite (e.g. Bostick and Fendorf, 2003; Han et al., 2013; Bulut et al., 2014; this study). Among common iron sulfides, pyrite seems most capable of incorporating arsenic into the crystal lattice either by substitution of As (-I) for sulfur or As(III) for iron, or both (Simon et al., 1999; Savage et al., 2000; Deditius et al., 2008, 2014; Qiu et al., 2017; Le Pape et al., 2017). However, Blanchard et al. (2007) concluded that it is energetically more favorable at low temperature for arsenic to substitute for sulfur as opposed to iron in pyrite. Finally, the recently recognized retrograde solubility of arsenic in pyrite (Deditius et al., 2014) is consistent with the lowest temperature pyrite being able to accommodate the most substitution of arsenic into its crystal lattice.

In addition to arsenic, a number of other trace elements occur in natural pyrites, including low temperature "sedimentary", hydrothermal, and magmatic/metamorphic pyrites (Abraitis et al., 2004). For example, gold occurs as both nanoparticles as well as substitute at the atomic level in arsenian pyrite in Carlin-type gold deposits of Nevada, USA (Reich et al., 2005; Deditius et al., 2014). However, for low-temperature "sedimentary" pyrites, Co, Ni, and to a lesser extent, Cd, Cu, Mo, and Sb apparently are the most common associated trace elements in arsenic-bearing low-temperature pyrites (Huerta-Diaz and Morse, 1992; Saunders et al., 1997; Houben et al., 2017; Bonnetti et al., 2017). The arsenic concentrations in natural "sedimentary" pyrites (including pyrite in coal) is highly variable and has been documented as high as 8% (Kolker et al., 2001, 2003), but most sedimentary pyrites typically have < 1 wt.% arsenic (Kolker et al., 2001). Authigenic pyrites demonstrably formed by precipitation from natural groundwaters typically have less than ~1 wt.% arsenic, although a semi-quantitative (SEM-EDS) analysis by Pi et al. (2016) indicated that pyrite contained 4.9 wt.% arsenic. Electron microprobe analyses of coarse-grained pyrite formed by SRB in a Holocene clastic river floodplain aquifer in Alabama, USA (Fig. 2) indicate it contains up to 0.62 wt.% arsenic (Saunders et al., 2005b). Similarly, electron microprobe data from Lowers et al. (2007) documented authigenic pyrite with up to 1.1 wt.% arsenic in clastic Holocene aquifers in Bangladesh, and Houben et al. (2017) found a maximum of 0.37 wt.% arsenic (mean of 0.08 wt.%) in authigenic pyrite in a post-glacial (Holocene) clastic aquifer in northeastern Germany. Price and Pichler (2006) documented authigenic pyrite with up to 1.2 wt.% arsenic (average of 0.23 wt.%) in the Oligocene Suwannee limestone of western Florida, USA. In a recent study

by Bonnetti et al. (2107), pyrite from low-temperature sedimentary/biogenic uranium ore from China contained varying amounts of arsenic depending on its morphology and interpreted origin. For example, pyrite that formed by replacing organic matter contained a median arsenic content of ~ 0.95 wt.%, whereas framboidal pyrite had a median arsenic content of 0.22 wt.%, and euhedral pyrite octahedra had a median arsenic content of 0.036 wt.%. Finally, arsenian pyrite produced in lab experiments utilizing SRB by Kirk et al. (2010) contained 0.2 to 0.94 wt.% arsenic.

Published research has shown that arsenic contents of authigenic pyrite are variable, and perhaps this is best illustrated by a single biogenic arsenian pyrite grain shown in Saunders et al. (2005b) from their fluvial Alabama field site, similar to the one in Fig. 2. Secondary ion mass spectrometry (SIMS) was used to analyze a single $\sim 1.7\,\mathrm{cm}$ -diameter pyrite crystal traversing from the core to rim (17 analyses over 0.8 cm). Each spot analysis yielded paired $8^{34}\mathrm{S}$ and As/S ratio values (lacking a standard for arsenic on the SIMS, As/S ratio was used as a proxy for changing arsenic concentration in the pyrite). Results show that arsenic is most enriched in the core of the pyrite grain, similar to that shown in Fig. 2, and the arsenic-rich core correlates well with the lightest $\delta^{34}\mathrm{S}$ values. Saunders et al. (2005b) interpreted that data to be consistent with the onset of biogenic sulfate reduction causing arsenic removal from groundwater in the growing pyrite grains.

2. Methods

To test the concept that the stimulation of SRB to make pyrite can be an effective technique for remediating arsenic-contaminated groundwater, we selected an industrial site in northern Florida to attempt a field demonstration in groundwater that was moderately reducing and had pH values of 5 to 7 initially. Arsenic-bearing herbicide had been used at the site decades earlier, and previous remediation efforts at the site included contaminated-soil removal and an extensive "pump-andtreat" groundwater remediation approach. Previous efforts reduced the aerial extent and stabilized the plume, and reduced dissolved arsenic concentrations to $\sim 0.3-1 \text{ mg/L}$ (Lee at al., accepted). For this investigation, four new wells were installed: two injection wells paired with two nearby (~1.5 m down gradient) monitoring wells to augment six other existing monitoring wells farther down gradient at the site (Lee et al., accepted). In early February 2016, we injected 11,730 L of aqueous solution containing molasses, agricultural-grade ferrous sulfate (FeSO₄•7H₂O), which together provided SRB a carbon source and the iron and sulfur needed to make pyrite. Further, 2 kg of agricultural grade diammonium phosphate was also added to the injection solution as well to provide a source of nitrogen and phosphorus nutrients for bacteria, and to also supply chloride (a minor constituent of the diammonium phosphate) for use as a tracer for groundwater flow (Lee et al., accepted). Groundwater samples were collected weekly from the two injection wells and eight monitoring wells after the injection of the bacteria-stimulating solution for the first month and then monthly

For the pyrite arsenic-sorption experiments, coarsely crystalline hydrothermal pyrite was crushed to several size fractions for use in arsenic-sorption experiments conducted in an anaerobic chamber under variable pH conditions and arsenic concentrations. Although our field demonstration project involved the formation of "biogenic" pyrite, we chose to use pyrite that was *not* formed by bacterial action for our sorption experiments so as to preclude the possibility that bacteria could enhance the inorganic sorptive capability of pyrite. The initial pH was adjusted with HCl and NaOH. It was not corrected during experiments, but the pH of the final solution/supernatant was then measured. Before transporting inside the anaerobic glove box, all aqueous solutions were prepared in doubly deionized water and purged for 3 h with ultrapure N_2 . Oxygen levels in the glove box and aqueous solutions were measured by Strathkelvin Oxygen meter (detection limit is $2.0 \pm 1 \, \mu mol/L$; $< 1 \, ppm$) to monitor O_2 levels. Arsenic stock

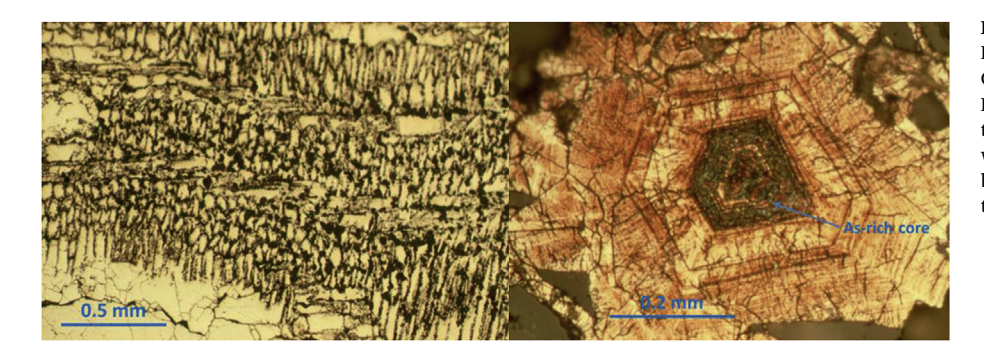


Fig. 2. Photomicrographs (reflected light) of Holocene biogenic arsenian pyrite from Macon County, Alabama (See Saunders et al., 1997, 2005b). LEFT: Pyrite replacing wood and preserving cellular textures. RIGHT: A single crystal of pyrite etched with a solution of HCl-KMnO $_4$ to show growth banding, and which also serves to preferentially stain the most As-rich zones.

solutions were prepared by dissolution of arsenic trioxide powder $(As_2O_3, 99.95\%)$; Fisher Chemicals) for two days in deoxygenated doubly deionized water inside the anaerobic chamber following procedure from Farquhar et al. (2002). Experiments conducted to calibrate equilibrium adsorption time ran for 72 h. Aliquots of the aqueous solutions were analyzed by graphite-furnace AA in the Department of Civil Engineering at Auburn University.

In the demonstration experiment at the industrial site field geochemical parameters were measured (including dissolved concentrations of H₂S and arsenic species), and aqueous sample collection and storage were conducted following standard EPA and USGS protocols. See Lee et al. (accepted) for details of well locations, aqueous geochemical sampling techniques and complete results of the pre- and postinjection site groundwater geochemical conditions. But in short, aqueous samples were then analyzed by ICP-MS (Agilent 7900) in the Department of Geoscience at Auburn University for major ions and (total) arsenic, and the major anions were analyzed using ion chromatography by a commercial lab. Suspended biogenic pyrite grains were collected from the bottom of monitoring wells, frozen in the field using CO2-ice, and were then transported to a freezer in the lab. Subsequently, these samples were thawed at room temperature, and the heavier sulfide phases were separated out by use of a centrifuge and then dried. The sulfide concentrates were then characterized by X-ray diffraction (XRD), and X-ray fluorescence (XRF), scanning electron microscopy (SEM), optical microscopy, and electron microprobe at Auburn University. Sulfur isotope signatures of dissolved sulfate were measured to fingerprint the progress of bacterial sulfate reduction in treated groundwater. Dissolved sulfate in groundwater was precipitated as $BaSO_4$, after spiking solutions with $BaCl_2$. The $\delta^{34}S$ values of the BaSO₄ were measured at the Colorado Plateau Stable Isotope Analysis Laboratory at Northern Arizona University, and δ^{34} S values of pyrite aggregates were measured by Geochron Laboratories, Chelmsford, MA.

3. Results

3.1. Arsenic sorption by pyrite

To address grain size influences of pyrite crystals to arsenic sorption, and shed more light on whether or not pyrite formed during biogenic sulfate reduction would continue to sorb arsenic in sulfur limited or sulfur depleted groundwater environments, we endeavored to conduct laboratory experiments. Because published iron-sulfide arsenic-adsorption experiments used very fine-grained synthetic pyrite (Bostick and Fendorf, 2003; Kim and Bachelor, 2009; Han et al., 2013) or mackinawite (FeS), which is a ubiquitous precursor to pyrite, (Gallegos et al., 2007; Jeong et al., 2010), we conducted laboratory batch experiments to evaluate natural pyrite sorption capabilities. Results show that (ground) natural pyrite is an effective adsorber of As (III), finer grain size with higher surface areas works the best, and sorption data fits reasonably well with Langmurian behavior ($r^2 > 0.988$) (Fig. 3). Results from this study show that arsenic sorption onto pyrite approaches a plateau at higher aqueous concentration.

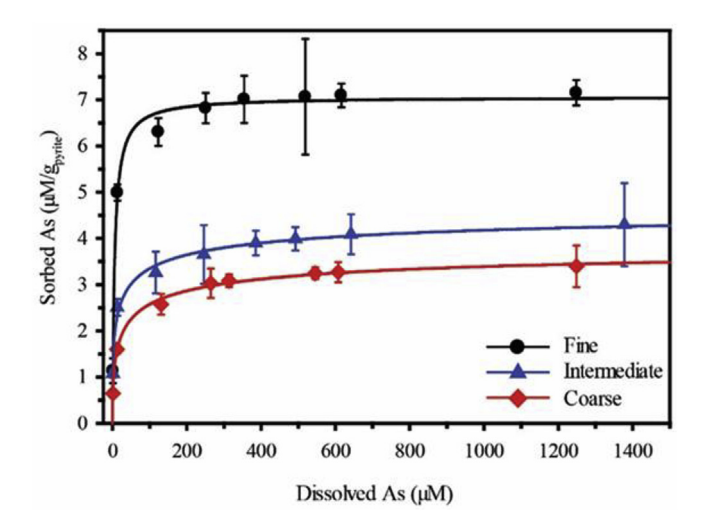


Fig. 3. Plot showing prediction of arsenic adsorption isotherm at pH 7 for fine, intermediate and coarsen-grained pyrite (6 g/L) (Ionic Strength = $0.01\,M$) fitted to Langmuir sorption model. Coefficient of determination, r^2 for the best Langmuir fit on the dataset presented here are 0.9885, 0.9849, and 0.995 for fine-, intermediate-, and coarse-grained samples, respectively. Vertical bars show standard deviations of the data.

Notably, arsenic sorption onto pyrite have shown to increase with elevated dissolved arsenic concentration indicating importance of pyrite in arsenic removal (Kim and Bachelor, 2009; Bulut et al., 2014).

The pH envelopes for arsenic on pyrite indicate that sorption increases with increasing pH, particular at pH > 5 and at elevated dissolved arsenic concentration (Fig. 4). Previous studies have shown comparable edge positions, and pH dependence of arsenic sorption onto pyrite (Bostick and Fendorf, 2003). The pH dependence of As sorption onto pyrite is distinctly different from other research conducted to study arsenic adsorption onto iron (oxy)hydroxides. One common reason for such contrast argued in earlier studies is that arsenic makes a strong inner-sphere complex with metal sulfide, unlike anion sorption onto iron (oxy)hydroxides is essentially through ligand-exchange of surface hydroxyl group (Bonnissel-Gissinger et al., 1998). Additionally, increase in arsenic sorption can also be explained by formation of ≡ Fe-OH surface sites which are the primary functional groups on the pyrite surface at higher pH levels (Chapelle and Lovley, 1992). Both innersphere complexation, and metal surface site functional groups are thus probably involved in the sorption of As onto pyrite, providing stable bond for long term arsenic retention. Finally, the arsenic sorption data suggest that the process might continue even after biogenic sulfate reduction ends, depending on the amount of pyrite formed in the aquifer and the residual and arsenic concentration in groundwater.

3.2. Initial results of field arsenic-bioremediation project

Pre-injection "background" geochemical conditions and the post-

Applied Geochemistry 96 (2018) 233-243

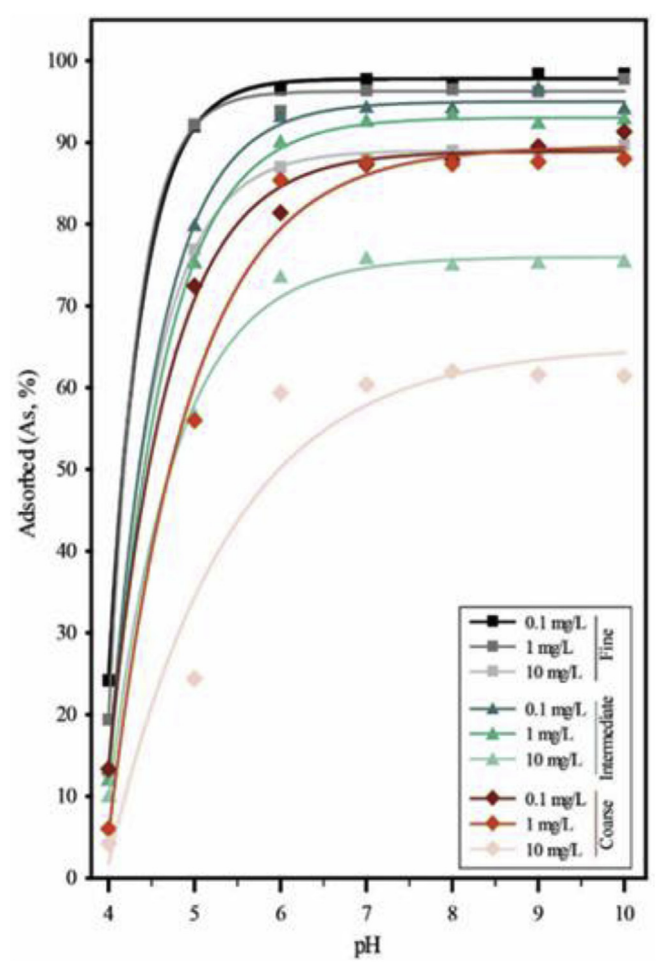


Fig. 4. Plot showing sorption envelope exhibiting Langmuir sorption behavior for different arsenic concentrations (1.35, 13.35, 133.45 μ M) on 6 g/L of fine, intermediate, and coarse-grained pyrite suspension (Ionic Strength = 0.01 M) equilibrated for 36 h modeled with best-fit curves.

injection changes during the entire 12-month field project are documented in detail in Lee et al. (accepted). Background groundwaters contained 0.1–1 mg/L, which predominantly occurred as the arsenite (As(III)) species. At the first weekly sampling of at the field site after injection of the groundwater amendments, a $\rm H_2S$ smell was present and ORP values dropped below $\rm -150~mV$ in the injection wells and paired monitoring wells, and arsenic started to decrease in the samples. After $\rm \sim 30~days$ the site regulatory clean-up goal of 0.05 mg/L had been reached and has remained below that for 6 months (Fig. 6). We should note that the regulatory clean-up goal for this site was based on the earlier USA EPA Drinking Water standard of 0.05 mg/L (pre-2000) and thus it does not necessarily represent current site regulatory goals in USA.

Injection of the bacteria-stimulating solution led to an expected increase in dissolved sulfate and iron in groundwater during the first two weeks, followed by a spike in H_2S in week 3 (Fig. 5). The concurrent decrease in iron, sulfate, and arsenic in the third week, followed by decrease in H_2S in the 4th week, appears to be related to SRB metabolism leading to the precipitation of pyrite and removal of arsenic from groundwater. It is possible that a slight and temporary increase observed for arsenic in week 3 could have been caused by competition of injected PO_4 with arsenic on mineral-sorption sites, which has been documented previously (e.g., Campos, 2002), although recent research suggests that arsenic-phosphate sorption relations are complex (Aziz et al., 2017). Another possibility is that elevated levels of dissolved H_2S produced at the initiation of biogenic sulfate reduction led to the

transient formation of aqueous thioarsenite complexes (e.g., Wilkin et al., 2003). After injection of the bacteria-stimulating solution, groundwater Eh dropped as expected, allowing SRB to out-compete Fe (III)-reducing bacteria for the electron donor organic carbon (e.g. Chapelle and Lovley, 1992). Paired Eh-pH values of groundwater corresponding to pre-injection conditions and subsequent values one month later (Fig. 6) record the drop in Eh. Prior to the injection of amendments, groundwater Eh-pH values plotted in the stability field of arsenite (As(III), As(OH)3°), whereas one month after injection of the solution, most values plotted in the stability field of arsenian pyrite (Fig. 6). Saunders et al. (2005b; 2008) and Ford et al. (2007) showed that for moderately reducing, circum-neutral pH groundwaters, the stability field of As(OH)3° generally overlaps with the field of Fe(II), consistent with their occurrence under bacterial Fe(III)-reducing conditions (e.g. Chapelle and Lovley, 1992).

3.3. Arsenian-pyrite formation during bioremediation

During the field bioremediation experiment, suspended iron-sulfide particles began to form at the bottom of the monitoring wells, which we were able to collect using a small peristaltic pump. Some of this material was mounted in epoxy and polished for optical (reflected light) microscopy and electron microprobe analyses, whereas and other splits were directly used for SEM, XRD and XRF analyses. Polished sections of the iron-sulfide grains were used for electron microprobe analyses.

Optical investigations indicated that only individual pyrite euhedra and framboid aggregates were present (e.g. no marcasite, mackinawite, or apparent amorphous iron-sulfide phases were visible). This observation was confirmed by XRD patterns that were similar to arsenian pyrite described from a lignite mine in the Czech Republic (Rieder et al., 2007). SEM imaging confirmed optical results with regards to the occurrence of both euhedral pyrite crystals and framboids composed of smaller euhedral nanocrystals of pyrite (Fig. 7). The bulk of pyrite crystals and framboids are typically $\sim 1-10 \, \mu m$ in diameter (Fig. 7). All of the monitoring wells sampled contained both the pyrite euhedra and framboids. Thus there was no apparent spatial control on their distribution. The co-occurrence of both types of authigenic pyrite morphologies in natural groundwater environments has been observed by others (Price and Pichler, 2006; Lowers et al., 2007; and Houben et al., 2017), and also in pyrite-bearing sedimentary biogenic uranium ores (Bonnetti et al., 2017). XRF analyses of the same powder samples used for XRD confirmed the presence of arsenic in the bulk samples (Fig. 8), and that result was corroborated by electron microprobe analyses of arsenic in individual pyrite crystals and framboids (Fig. 8). Electron microprobe analyses indicates that the biogenic arsenian pyrite contains ~ 0.05 to 0.4 wt.% (500–4000 mg/kg) of arsenic, which are within the reported ranges of arsenic in pyrite from natural groundwater environments (Saunders et al., 2005b, Price and Pichler, 2006; Lowers et al., 2007; and Houben et al., 2017). We observed no apparent relation in the arsenic content of the two different pyrite morphologies that formed during the field bioremediation experiment. However, Lowers et al. (2007) observed that single ("massive") pyrite crystals had significantly higher concentrations of arsenic than did framboids (e.g., mean values 2x as much).

Individual pyrite crystals formed during the bioremediation field experiment are typically modified octahedrons, some of which exhibit twinning (Fig. 8). Framboids appear to be aggregates of much smaller euhedral (octahedral?) crystals. Houben et al. (2017) described individual pyrite crystals formed in a post-glacial (Holocene) aquifer as having cubic, octahedral, cubo-octahedral, and rhombic dodecahedral morphologies, and that framboids were aggregates of euhedral octahedral crystals. Houben et al. (2017) suggested that individual pyrite crystals may have formed by the recrystallization of the framboids. We have seen no evidence of that process in our field experiment, where both single crystals and framboids appear to have both formed at the same time. Further, Southam and Saunders (2005) observed that early

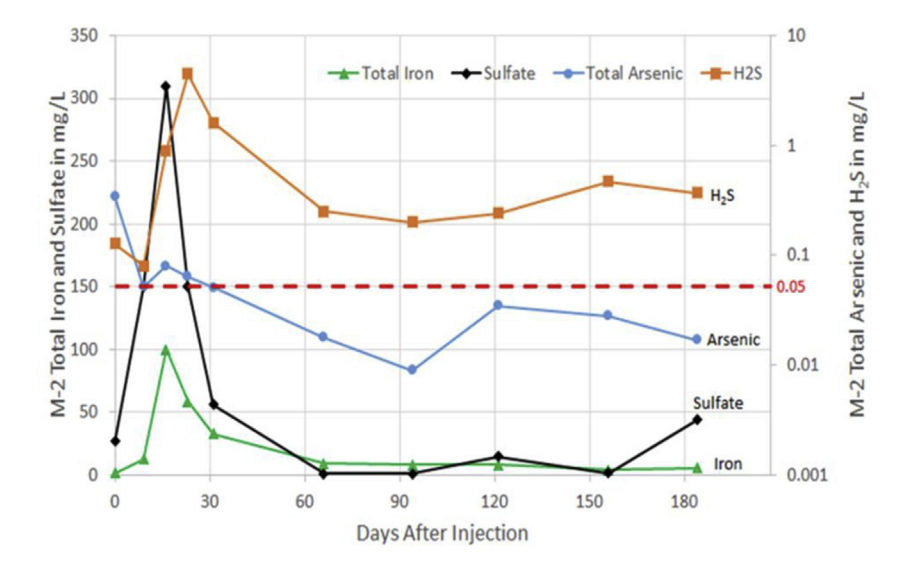


Fig. 5. Plot showing time-series groundwater geochemical data (dissolved) from a monitoring well (M-2) at the Florida industrial site, showing pre-injection geochemical conditions and subsequent changes during the first 6 months of the bioremediation field experiment. Time-related decreases in Fe, H_2S , and As are interpreted here to be the result of precipitation of arsenian pyrite. Dashed red line is the regulatory cleanup goal for arsenic concentration at the field site. The complete 12-month aqueous geochemistry data set for all 10 wells periodically sampled in the field demonstration project is presented in Lee et al. (accepted). (For interpretation of the references to colour in this figure legend, the reader is referred to the Web version of this article.)

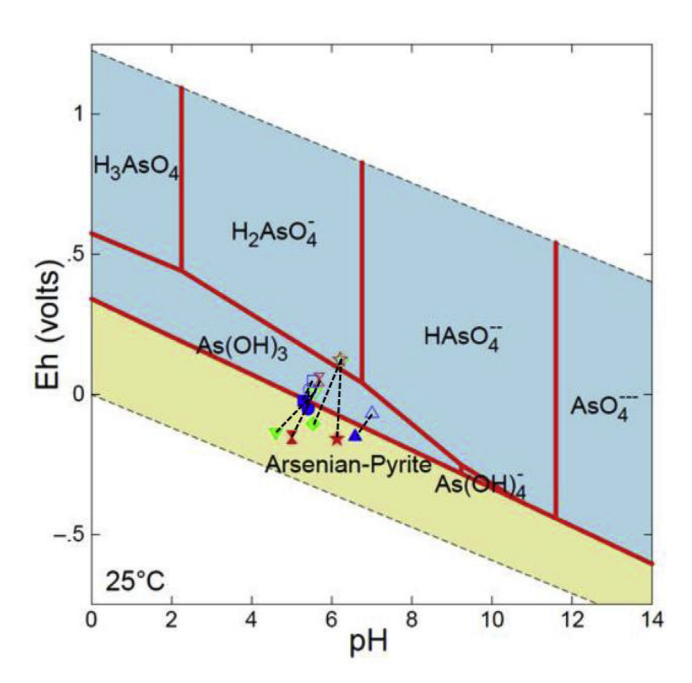


Fig. 6. Eh-pH diagram calculated for As-Fe-S-H₂O system at 25 °C and fixed As, Fe²⁺, and SO_4^{2-} activities of 10^{-6} , 10^{-4} , and 10^{-5} , respectively. The results show the stability field of different arsenic species under different geochemical condition. Also plotted are the Eh and pH values of groundwater measured in monitoring wells for both pre-injection conditions (open symbols) and then for one month after the injection (solid symbols). Plot was constructed using Geochemist's Workbench including thermodynamic data listed in the Appendix.

(biogenic) framboidal pyrite textures were preserved after later encrustation by coarser-grained pyrite in a Holocene aquifer, suggesting that at least in some situations, pyrite framboids don't necessarily recrystallize to form euhedral pyrite crystals. According to Wilkin and Barnes (1996), the formation of framboidal pyrite is apparently favored when iron monosulfides rapidly convert to pyrite. If that interpretation is correct, then perhaps in our field experiment, framboidal pyrite formed by recrystallization of an iron monosulfide precursor, and the euhedral octahedral pyrite crystals formed from direct precipitation from groundwater during sulfate reduction.

3.4. Sulfur isotopes

Given the small size of pyrite grains formed during the bioremediation field experiment, it is difficult to determine the approximate δ^{34} S value for individual grains. For example, the typical beam size for an ion microprobe (SIMS) is $\sim 20 \, \mu m$, which is about $\sim 4x$ larger than the average pyrite crystal or framboid observed in this study (Fig. 9). Thus we analyzed (using conventional S-isotope combustion techniques) composite samples of pyrite grains taken from three different monitoring wells undergoing biogenic sulfate reduction. Results of the three analyses in terms of $\delta^{34}S$ (CDT) were -5.3, -6.7, and -11.7%, which are values generally consistent with typical marine pyrites formed by biogenic sulfate reduction (e.g. Ohmoto and Goldhaber, 1997; Seal, 2006), and those values overlap the range observed for Holocene biogenic pyrite like that shown in Fig. 2, which have a mean δ^{34} S of -13.5% (n = 17; Saunders et al., 2005b). Further, a detailed sulfur isotope study conducted on pyrite interpreted to have formed as a consequence of SRB metabolism from a Chinese sedimentary uranium deposit (Bonnetti et al., 2017) contained even isotopically lighter δ^{34} S

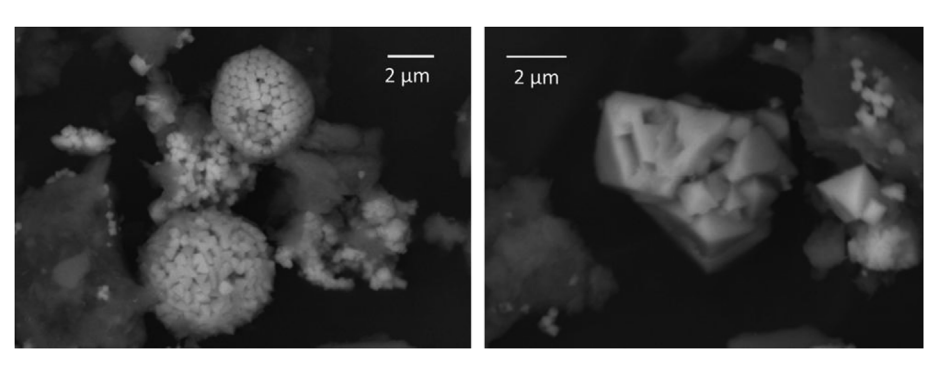


Fig. 7. SEM backscatter images of biogenic arsenian pyrite crystal (right) and framboids (left) and associated aquifer silicate minerals (grey) that formed during the first few months of the bioremediation experiment.

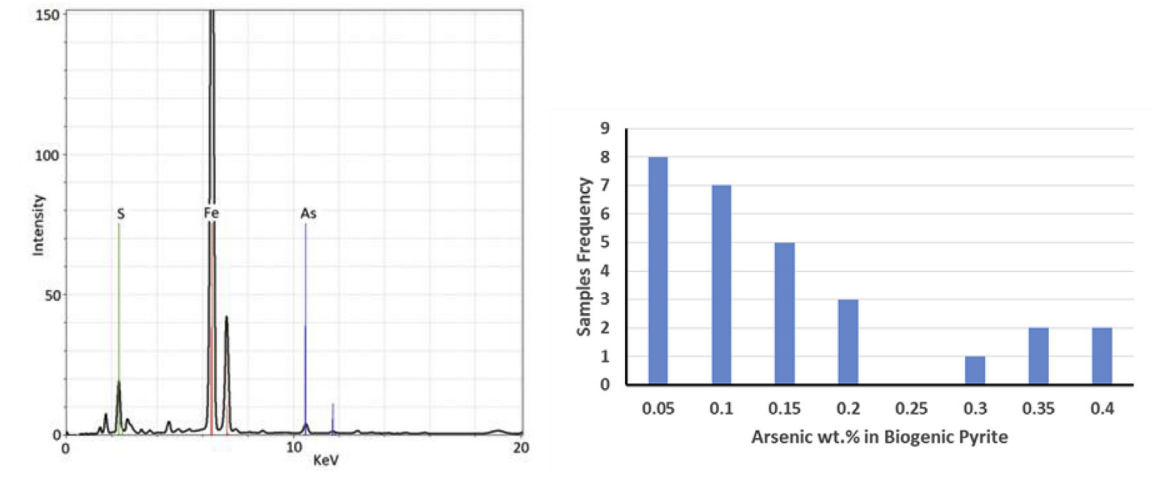


Fig. 8. LEFT: XRF spectrum showing peaks for Fe, S, and As from a composite sample of pyrite grains similar to those shown in Fig. 7, which formed in the first month of the field bioremediation experiment. RIGHT: Histogram showing electron microprobe results of arsenic concentrations of individual pyrite grains formed during bioremediation.

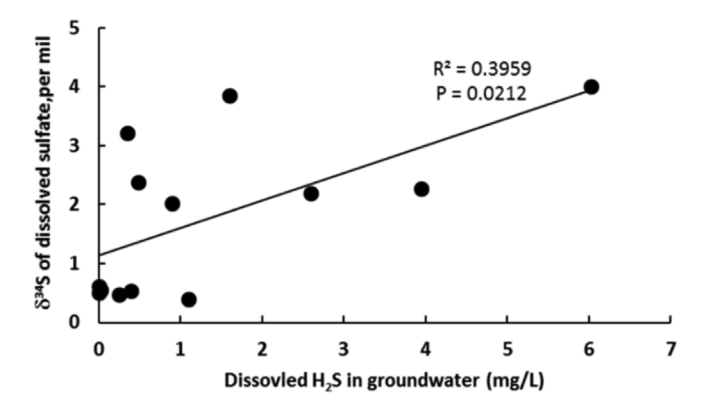


Fig. 9. Plot of $\delta^{34}S$ (CDT) of dissolved sulfate vs. concentration of $H_2S_{\rm aq}$ for groundwater in the field bioremediation experiment.

values. There, framboidal pyrite in the uranium ore had a mean δ^{34} S value of -38.9% and pyrite that apparently formed by replacing solid organic matter had a mean δ^{34} S of -24.2% (Bonnetti et al., 2017).

The $\delta^{34}S$ values of dissolved sulfate (Fig. 9) are consistent with bacterial-sulfate reducing conditions. The $\delta^{34}S$ of sulfate in the injection solution was $\sim 0.5\%$ (two analyses yielded 0.44% and 0.61%), and groundwater sulfate δ^{34} S values recorded during the bioremediation experiment increased to as much as 4.0%. This increase of $\sim 3.5\%$ is consistent with SRB reducing sulfate to H2S, which is enriched in the lighter isotope, which in turn reacts with dissolved iron to make pyrite that is enriched in 32 S (e.g. negative δ^{34} S values). There is essentially no fractionation of the δ^{34} S values of H₂S and pyrite formed in equilibrium with it at this temperature (Ohmoto and Goldhaber, 1997; Seal, 2006). Thus taken together, the increase in $\delta^{34}S$ values for dissolved sulfate coupled with a negative $\delta^{34}S$ values of the neo-formed pyrite are evidence of biogenic sulfate reduction during the bioremediation experiment. The apparent relatively small depletion of sulfide δ^{34} S values (for bacterial sulfate reduction) as compared to starting sulfate values (\sim 10–15‰) could be the result of either very rapid sulfate reduction in this study, the "open system" conditions of having excess dissolved sulfate, or both (e.g., Seal, 2006).

4. Discussion

The concept of remediating water contaminated by arsenic by causing it to precipitate as an arsenic-bearing mineral is not new. For example, dissolved arsenic in pore waters has been lowered by engineering the precipitation of scorodite from pore waters in contact with uranium mine tailings in Saskatchewan (Langmuir et al., 2006). There, arsenic-bearing mine tailings are being treated by back-filling them in abandoned mine-pit lakes. Amorphous and crystalline scorodite are fairly soluble, thus forming these phases leaves significant arsenic in solution, but this technique has garnered regulatory approval in Canada (Langmuir et al., 2006). In the USA, contaminated-site remediation goals are largely driven by drinking water standards (DWS). The groundwater DWS (US EPA and World Health Organization, WHO) for arsenic is 10 ug/L, and thus precipitation of the relatively soluble mineral scorodite would not lower dissolved arsenic concentrations to levels needed for regulatory acceptance of that concept. Sulfide minerals typically have much lower solubility than the corresponding oxides, oxyhydroxides, carbonates, or sulfates of a particular metal (loid) (Langmuir, 1997). Thus, groundwater remediation strategies perhaps should be focused on removing As in sulfide minerals (e.g. Keimowitz et al., 2007; Saunders et al., 2008). This approach has worked well for bioremediating metal-contaminated groundwaters (Lee and Saunders, 2003; Saunders et al., 2005a, 2008). However, crystalline or amorphous arsenic-sulfide phases are more soluble than sulfides of chalcophile metals such as Pb, Zn, Cd, etc. (Langmuir, 1997) and thus arsenic removal by forming sulfide phases is not straight forward. For example, if precipitation of orpiment is the goal for utilizing SRB in bioremediation of arsenic-contaminated groundwater, our modelling suggests that would not be viable for circum-neutral-pH groundwaters (Fig. 10). A groundwater of pH 6 and $\sim 10^{-4.8}\,\mathrm{M\,H_2S}$ (e.g., approximate conditions for the groundwater in shown in Fig. 6 at 180 days) in equilibrium with amorphous orpiment would have a dissolved arsenic value of $\sim 10^{-4.5}$ M (~ 2 mg/L; Fig. 10). If less soluble crystalline orpiment could be formed, that would lower the expected remaining arsenic in solution but would not enough to approach desired clean-up goals or drinking water standards.

For modelling purposes, adding iron to the As- $\rm H_2S$ - $\rm H_2O$ system complicates interpretation and implications for arsenic remaining in solution after precipitation of iron-arsenic sulfides. In particular, there is a lack of thermodynamic data for arsenian pyrite of varying arsenic content, and there are uncertainties about whether crystalline arsenopyrite will form under low-temperature groundwater conditions. Saunders et al. (2008) estimated ΔG_f values for arsenian pyrite of varying arsenic contents based on one published lab experiment, and modelling using that data indicated arsenian pyrite (with 1 wt.% arsenic) displaces the stability fields of orpiment and realgar in Eh-pH space. Modelling by Langner et al. (2013, supplementary information) using arsenopyrite as the preferred reduced arsenic-bearing iron-sulfide

Applied Geochemistry 96 (2018) 233-243

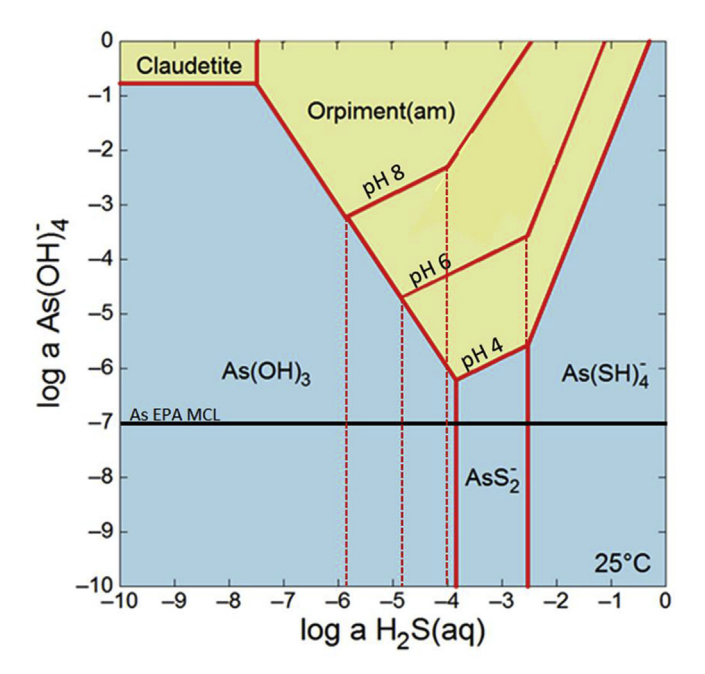


Fig. 10. Activity-activity diagram for the As-H₂S system calculated using Geochemist's Workbench and thermodynamic data in the Appendix, for varying pH values. Dashed vertical lines represent the shifting stability boundaries of the field of aqueous AsS₂⁻ with varying pH values. Results show that the stability field of amorphous orpiment expands at lower pH values (e.g., consistent with conditions of acid mine drainage).

phase also displaced the stability field of orpiment and realgar in Eh-pH space. However, the reported occurrences of low-temperature amorphous or crystalline arsenopyrite need further substantiation by XRD. Indeed, in some arsenic-rich hydrothermal ores such as Carlin-type gold deposits, temperatures of ore formation may have been too low even in those to form arsenopyrite in those systems, as arsenian pyrite (not arsenopyrite) hosts gold in those deposits (Deditius et al., 2014; Saunders et al., 2014). However, arsenopyrite is a common mineral associated with higher-temperature hydrothermal ores (Saunders et al., 2014). Thus, based on natural occurrences of arsenian pyrite reported in most natural groundwater systems, we proposed that it is the phase to target for precipitation for arsenic-sequestration during bioremediation of arsenic-contaminated groundwater using SRB. The common situation in many groundwaters contaminated by either anthropogenic or natural arsenic sources is that dissolved Fe(II) exceeds dissolved arsenic and thus, arsenic-bearing iron sulfides likely are more important at circum-neutral pH than arsenic-only sulfides (Saunders et al., 2008), which has been documented in numerous studies cited

The stimulation of SRB to make H₂S_{aq} during bioremediation must overcome the effect of the formation of aqueous thioarsenite complexes that can form at elevated H_2S_{aq} concentrations (Wilkin et al., 2003). Keimowitz et al. (2007) and Sun et al. (2016) observed this effect on arsenic mobility in their laboratory experiments involving SRB. Sun et al. (2016) utilized mine tailings from two different sites as substrates for experiments designed to stimulate SRB metabolism by addition of an organic carbon source (lactate) ± sulfate. Omoregie et al. (2013) conducted similar microcosm experiments, but for their substrate, they used aquifer sediments that host naturally arsenic-contaminated groundwater from Cambodia. Omoregie et al. (2013) showed that significant amounts of arsenic were removed by forming iron-arsenicsulfide phases, but that the resulting remaining solution still contained arsenic concentration of $\sim 30 \,\mu\text{g/L}$, which is higher than the WHO DWS of 10 µg/L. Experiments stimulating bacterial sulfate reduction coupled with iron-sulfide formation by Onstott et al. (2011) and Keimowitz

et al. (2007) were effective in removing significant amounts of dissolved arsenic, but also left $30\,\mu\text{g/L}$ and $22\,\mu\text{g/L}$ (respectively) arsenic in solution. Laboratory experiments by Kirk et al. (2010) showed that the formation of arsenian pyrite was important for removing dissolved arsenic, but their conditions did not produce enough of the mineral phase to dramatically decrease dissolved arsenic. In the only other published field study designed to stimulate SRB to remove arsenic by forming pyrite, Pi et al. (2017) reported that arsenic concentration in groundwater at their site dropped from 593 $\mu\text{g/L}$ to $136\,\mu\text{g/L}$. In their study, Pi et al. (2017) amended groundwater with ferrous sulfate and did not add a carbon electron donor to groundwater (as was done in this study).

The addition of iron to the As-H₂S system has several effects based on published data (e.g., Wilkin et al., 2003; Saunders et al., 2008; Burton et al., 2011, 2014; Kirk et al., 2010; Couture et al., 2010, 2013): 1) It lowers the dissolved concentration of H₂S by precipitating ironsulfides, which can limit the formation of thioarsenite complex that can increase arsenic mobility; 2) Addition of iron limits the stability fields of crystalline or amorphous solid arsenic-only sulfide phases and lead to formation of iron-arsenic sulfides; 3) Crystalline iron-sulfide phases mackinawite, greigite, and pyrite have all been shown to be capable of sorbing arsenic from solution; and 4) Precursor iron sulfides formed during biogenic sulfate reduction may have inverted to the thermodynamically most stable phase pyrite; subsequently arsenic sorbed onto former surfaces can be incorporated by substitution for sulfur and perhaps iron in pyrite (Wolthers et al., 2005a). During SRB metabolism, pH usually increases as protons are required to make H₂S from sulfate (Saunders et al., 2005a, 2008) and this aids in arsenic sorption on pyrite (see above). Thus our use of the term "sequestration" of arsenic in pyrite can be thought of as both a sorption, then coprecipitation process in pyrite, irrespective of whether pyrite had a poorly crystalline ironsulfide precursor or directly precipitated from solution. Perhaps both of these processes occurred during our field bioremediation experiment and would explain the simultaneous production of euhedral pyrite crystals and framboidal aggregates.

Iron sulfide minerals are stable under reducing geochemical conditions and thus their long-term stability is an issue for their formation during biogenic sulfate reduction. If the groundwater conditions remain reducing, the low solubility of pyrite means that it provides a long term stable sink for arsenic unless the pyrite is oxidatively dissolved (Wolthers et al., 2005a). So in general, due to the low solubility of O₂ in groundwater, iron sulfides are typically stable below the water table where they are out of direct contact with the atmosphere (Langmuir, 1997). Fluctuations of shallow water table levels due to a lack of rainfall is an issue that can lead to oxidation of previously precipitated sulfide minerals (Saunders et al., 2005a). Further, oxidation of disseminated arsenic-bearing sulfides in aquifers has been shown to contaminate groundwater with arsenic (Price and Pichler, 2006; Mango and Ryan, 2015; Houben et al., 2017). However, laboratory experiments by Onstott et al. (2011) designed to investigate the results of the oxidation of arsenic-bearing iron sulfides indicated that arsenic is not necessarily released to solution as it sorbed by the neo-formed ironoxyhydroxides caused by oxidation of iron sulfides. Thus, bioremediation using biogenic iron sulfides to remove arsenic in groundwater probably requires continued monitoring at sites, at least until longer term data becomes available on the stability of arsenic-bearing pyrite.

In summary, we show here that natural SRB can be stimulated to make biogenic pyrite in the field for circum-neutral pH groundwaters, and it appears that dissolved arsenic is sequestered by sorption and coprecipitation. A technique similar to that documented here could prove effective where groundwater is contaminated by acid mine drainage, but sorption behavior on iron-sulfide minerals, and the resulting mineralogy could be substantially different at lower pH, although SRB metabolism does cause pH to increase (Saunders et al., 2008). However, most *naturally* arsenic-contaminated groundwaters such as in Southeast Asia and elsewhere typically occur under circum-

neutral pH and moderately reducing conditions similar to the site in this study. Thus we envision that this process perhaps can be modified to treat individual wells where arsenic-contaminated groundwater is abstracted. Both the long-term stability of the reducing geochemical conditions resulting from bioremediation and the stability of the arsenian pyrite with time warrant additional study.

5. Conclusions

The principal conclusion is that bioremediation of arsenic-contaminated groundwater can be accomplished by stimulating indigenous SRB to make arsenian pyrite. Optimization of the process is needed on a site-specific basis where geochemical conditions (i.e., Eh-pH, concentrations of iron, sulfate, and organic carbon) vary from our field site. A preliminary conclusion from our study along with other published lab and field studies is that formation of abundant arsenian pyrite will be most effective in removing arsenic from solution, but too much pyrite formation could reduce aquifer permeability and porosity. Other conclusions and implications are listed below:

- Arsenic-only sulfides may be more important mineral phases that could form at lower pH conditions related to anthropogenic conditions such as related to acid mine drainage. However, even in that situation, there will be high levels of dissolved iron in the system and thus arsenic-bearing iron sulfides are more likely the authigenic mineral phases formed.
- 2) To optimize arsenian pyrite formation during bioremediation, both ferrous iron sulfate and a labile source of organic carbon should be used to amend groundwater.
- Amending groundwater with ferrous iron, besides aiding in pyrite formation and growth, limits the formation of thioarsenite complexes, which can enhance arsenic mobility under reducing conditions.

- 4) Arsenic sequestration appears to have been caused by an initial sorption onto pyrite nanoparticle surfaces, and as the pyrite crystals grew over the first few months of the bioremediation experiment, previously sorbed arsenic apparently was incorporated in pyrite by substitution for sulfur. Depending on the amount of dissolved arsenic in the system, and the amount of biogenic pyrite produced during bioremediation, there could be a residual effect of continued sorption of arsenic by pyrite after bacterial sulfate reduction ends. Because we sampled the groundwater seven days after the injection solutions were added, we cannot rule out the possibility that mackinawite or amorphous iron sulfide could have formed rapidly, sorbed some of the dissolved arsenic, and inverted to crystalline pyrite prior to our first sampling, although we saw no evidence of that.
- 5) Biogenic sulfate reduction leads to an increase in pH, which as shown here will enhance arsenic sorption on pyrite surfaces.
- 6) Finally, in "developed" nations, it is highly unlikely that shallow groundwater from contaminated industrial sites like that described here will ever be used for drinking water. However, in developing nations where natural arsenic contamination of their potable groundwater supplies is a problem, it is possible that in situ treatment using the concepts presented here might prove useful in lowering the arsenic content of drinking water there (and perhaps very inexpensively).

Acknowledgements

This research was supported by a grant from the National Science Foundation (NSF-1425004) to James Saunders, Ming-Kuo Lee, and Ashraf Uddin. NSF had no role in the study design, collection, analysis and interpretation of data, or in the writing and submission of this paper.

Appendix

Equilibrium constants (at 25 °C) for the formation of thioarsenites, arsenic sulfides, iron sulfides, and arsenian pyrite used in geochemical modelling.

Reactions	$\log K_{25}$	References
Thioarsenite species		
$As(OH)_4^- + HS^- + 2H^+ \Leftrightarrow As(OH)_2(SH) + 2H_2O$	17.92	Wilkin et al. (2003)
$As(OH)_4^- + HS^- + H^+ \Leftrightarrow As(OH)_2S^- + 2H_2O$	12.77	Wilkin et al. (2003)
$As(OH)_4 + 2HS + H^+ \Leftrightarrow As(OH)S_2^{2-} + 3H_2O$	17.83	Wilkin et al. (2003)
$As(OH)_4^- + 3HS^- + 2H^+ \Leftrightarrow AsS_3H^{2-} + 4H_2O$	29.61	Wilkin et al. (2003)
$As(OH)_4 + 4HS + 4H^+ \Leftrightarrow As(SH)_4 + 4H_2O$	45.77	Wilkin et al. (2003)
$As(OH)_4 + 3HS + H^+ \Leftrightarrow AsS_3^{3-} + 4H_2O$	21.72	Wilkin et al. (2003)
Arsenic sulfides and iron sulfides		
$2As(OH)_4$ + $3HS$ + $5H$ $\Leftrightarrow As_2S_3$ (Orpiment) + $8H_2O$	65.60	Webster (1990)
$2As(OH)_4^- + 3HS^- + 5H^+ \Leftrightarrow As_2S_{3 \text{ (am)}} + 8H_2O$	63.27	Webster (1990)
$As(OH)_4^- + HS^- + 2H^+ \Leftrightarrow AsS (Realgar) + 3.5H_2O + .25 O_{2(ag)}$	14.68	Bethke (1996)
$Fe^{2+} + 2HS^{-} + .5 O_{2(aq)} \Leftrightarrow FeS_2 (Pyrite) + H_2O$	59.29	#
$.875 \text{ Fe}^{2+} + \text{HS}^{-} + .0625 \text{ O}_{2(aq)} \Leftrightarrow \text{FeS}_{.875}(\text{Pyrrhotite}) + .75 \text{ H}^{+} + .125 \text{ H}_{2}\text{O}$	9.88	#
$Fe^{2+} + HS^{-} \Leftrightarrow FeS (Mackinawite) + H^{+}$	3.10	Webster (1990)
$Fe^{2+} + As(OH)_4^- + HS^- \Leftrightarrow AsFeS (Arsenopyrite) + 2.5H_2O + .75 O_{2(ag)}$	-47.84	Bethke (1996)
Arsenian pyrite		
$FeS_{1.99}As_{0.01} + 1.02 H_2O + 3.5 O_2 (aq) \Leftrightarrow Fe^{2+} + 1.995 SO_4^{2-} + 0.01 As(OH)_4^{-} + 2H^{+}$	199.78	Saunders et al. (2008)

#Schoonen and Barnes (1991) and Wilkin and Barnes (1996).

References

textural and electrical properties of natural pyrite: a review. Int. J. Miner. Process. 74, 41–59.

Abraitis, P.K., Pattrick, R.A.D., Vaughan, D.J., 2004. Variations in the compositional,

Aziz, Z., Bostick, B.C., Zheng, Y., Huq, M.R., Rahman, M.M., Ahmed, K.M., van Geen, A., 2017. Evidence of decoupling between arsenic and phosphate in shallow

- groundwater of Bangladesh and potential implications. Appl. Geochem. 77, 167–177. Benning, L.G., Wilkin, R.T., Barnes, H.L., 2000. Reaction pathways in the Fe–S system below 100°C. Chem. Geol. 167, 25–51.
- Bethke, C.M., 1996. Geochemical Reaction Modeling. Oxford University Press, New York. Blanchard, M., Alfredsson, M., Brodholt, J., Wright, K., Catlow, C.R.A., 2007. Arsenic incorporation into FeS₂ pyrite and its influence on dissolution: a DFT study. Geochim. Cosmochim. Ac 71, 624–630.
- Bonnetti, C., Liu, X., Zhaobin, Y., Cuney, M., Michels, R., Malartre, F., Mercadier, J., Cai, J., 2017. Coupled uranium mineralisation and bacterial sulphate reduction for the genesis of the Baxingtu sandstone-hosted U deposit, SW Songliao Basin, NE China. Ore Geol. Rev. 82, 108–129.
- Bonnissel-Gissinger, P., Alnot, M., Ehrhardt, J.-J., Behra, P., 1998. Surface oxidation of pyrite as a function of pH. Environ. Sci. Technol. 32, 2839–2845.
- Bostick, B.C., Fendorf, S., 2003. Arsenic sorption on troilite (FeS) and pyrite (FeS₂). Geochem. Cosmochim. Acta 67, 909–921.
- Bostick, B.C., Fendorf, S., Brown, G.E., 2005. In situ analysis of thioarsenite complexes in neutral to alkaline arsenic sulphide solutions. Mineral. Mag. 69, 781–795.
- Bowell, R., Alpers, C.N., Jamieson, H., Majzlan, J., 2014. The environmental geochemistry of arsenic- an overview. Rev. Mineral. Geochem. 79, 1–16.
- Bulut, G., Yenial, U., Emiroglu, E., Sirkeci, A.A., 2014. Arsenic removal from aqueous solution using pyrite. J. Clean. Prod. 84, 526–532.
- Burton, E.D., Johnston, S.G., Bush, R.T., 2011. Microbial sulfidogenesis in ferrihydriterich environments: effects on iron mineralogy and arsenic mobility. Geochim. Cosmochim. Acta 75, 3072–3087.
- Burton, E.D., Johnston, S.G., Kocar, B.D., 2014. Arsenic mobility during flooding of contaminated soil: the effect of microbial sulfate reduction. Environ. Sci. Technol. 48, 13660–13667.
- Campos, V.F., 2002. Arsenic in groundwater affected by phosphate fertilizers at Sao Paulo. Brazil. Environ. Geol. 42, 83–87. https://doi.org/10.1007/s00254-002-0540-0
- Chapelle, F.H., Lovley, D.R., 1992. Competitive exclusion of sulfate reduction by Fe(III) reducing bacteria: a mechanism for producing discrete zones of high-iron groundwater. Ground Water 30, 29–36.
- Couture, R.-M., Gobeil, C., Tessier, A., 2010. Arsenic, iron, ad sulfur codiagenesis in lake sediments. Geochem. Cosmochim. Acta 74, 1238–1255.
- Couture, R.M., Rose, J., Kumar, N., Mitchell, K., Wallschlaeger, D., Van Cappellen, P., 2013. Sorption of arsenite, arsenate, and thioarsenates to iron oxides and iron sulfides: a kinetic and spectroscopic investigation. Environ. Sci. Technol. 47, 5652–5659.
- Deditius, A.P., Utsunomiya, S., Renock, D., Ewing, R.C., Ramana, C.V., Becker, U., Kesler, S.E., 2008. A proposed new type of arsenian pyrite: composition, nanostructure and geological significance. Geochem. Cosmochim. Acta 72, 2919–2933.
- Deditius, A.P., Reich, M., Kesler, S.E., Utsunomiya, S., Chryssoulis, S.L., Walshe, J., Ewing, R.C., 2014. The coupled geochemistry of Au and as in pyrite from hydrothermal ore deposits. Geochem. Cosmochim. Acta 140, 644–670.
- DeSisto, S.L., Jamieson, H.E., Parsons, M.B., 2016. Subsurface variations in arsenic mineralogy and geochemistry following long-term weathering of gold mine tailings. Appl. Geochem. 73, 81–97.
- Dixit, S., Hering, J.G., 2003. Comparison of arsenic(V) and arsenic(III) sorption onto iron oxide minerals: Implications for arsenic mobility. Environ. Sci. Technol. 37, 4182–4189
- Farquhar, M.L., Charnock, J.M., Livens, F.R., Vaughan, D.J., 2002. Mechanisms of arsenic uptake from aqueous solution by interaction with goethite, lepidocrocite, mackinawite and pyrite: an X-ray absorption spectroscopy study. Environ. Sci. Technol. 36, 757–1762.
- Fendorf, S., Michael, H., van Geen, A., 2010. Spatial and temporal variations of groundwater arsenic in South and Southeast Asia. Science 328, 1123–1127.
- Ford, R.G., Kent, D.B., Wilkin, R.T., 2007. Chapter 6, arsenic. In: Ford, R.G., Wilkin, R.T., Puls, R.W. (Eds.), Monitored Natural Attenuation of Inorganic Contaminants in Ground Water. U.S. EPA, pp. 57–70 Ada, OK, EPA/600/R-07/140.
- Gallegos, T.J., Hyun, S.P., Hayes, K.F., 2007. Spectroscopic investigation of the uptake of arsenite from solution by synthetic mackinawite. Environ. Sci. Technol. 41, 7781–7786.
- Giménez, J., María Martínez, M., de Pablo, J., Rovira, M., Duro, L., 2007. Arsenic sorption onto natural hematite, magnetite, and goethite. J. Hazard Mater. 141, 575–580.
- Godelitsas, A., Price, R.E., Pichler, T., Amendd, J., Gamaletsos, P., Göttlicher, J., 2015. Amorphous As-sulfide precipitates from the shallow-water hydrothermal vents off Milos Island (Greece). Mar. Chem. 177, 687–696.
- Han, J., Fyfe, W.S., 2000. Arsenic removal from water by iron-sulphide minerals. Chin. Sci. Bull. 45, 1430–1434.
- Han, D.S., Song, J.K., Batchelor, B., Abdel-Wahab, A., 2013. Removal of arsenite (As(III)) and arsenate(As(V)) by synthetic pyrite (FeS2): synthesis, effect of contact time, and sorption/desorption envelopes. J. Colloid Interface Sci. 392, 311–318.
- Houben, G.J., Sitnikova, M.A., Post, V.E.A., 2017. Terrestrial sedimentary pyrites as a potential source of trace metal release to groundwater - a case study from the Emsland. Germany. Appl. Geochem 76, 99–111.
- Huerta-Diaz, M.A., Morse, J.W., 1992. Pyritization of trace metals in anoxic marine sediments. Geochem. Cosmochim. Acta 56, 2681–2702.
- Jeong, H.Y., Han, Y.-S., Hayes, K.F., 2010. X-ray absorption and x-ray photoelectron spectroscopic study of arsenic mobilization during mackinawite (FeS) oxidation. Environ. Sci. Technol. 44, 955–961.
- Keimowitz, A.R., Simpson, H.J., Stute, M., Datta, S., Chillrud, S.N., Ross, J., Tsang, M., 2005. Naturally-occurring arsenic: mobilization at a landfill in Maine and implications for remediation. Appl. Geochem. 20, 1985–2002.
- Keimowitz, A.R., Mailloux, B.J., Cole, P., Stute, M., Simpson, H.J., Chillrud, S.N., 2007. Laboratory investigations of enhanced sulfate reduction as a groundwater arsenic

- remediation strategy. Environ. Sci. Technol. 41, 6718-6724.
- Kim, E.J., Bachelor, K., 2009. Macroscopic and X-ray photoelectron spectroscopic investigation of interactions of arsenic with synthesized pyrite. Environ. Sci. Technol. 43, 2899–2904.
- Kirk, M., Holm, T., Park, J., Jin, Q., Sanford, R., Fouke, B., Bethke, C., 2004. Bacterial sulfate reduction limits natural arsenic contamination in groundwater. Geology 32, 952–956
- Kirk, M.F., Roden, E.E., Crossey, L.J., Brealey, A.J., Spilde, M.N., 2010. Experimental analysis of arsenic precipitation during microbial sulfate and iron reduction in model aquifer sediment reactors. Geochem. Cosmochim. Acta 74, 2538–2555.
- Kolker, A., Nordstrom, D.K., Goldhaber, M.J., 2001. Occurrence and micro-distribution of arsenic in pyrite. In: USGS Workshop on Arsenic in the Environment, Denver, CO, Feb. 21–22.
- Kolker, A., Haack, S.K., Cannon, W.F., Westjohn, D.B., Kim, M.-J., Nriagu, J., Woodruff, L.G., 2003. Arsenic in southeastern Michigan. In: Welch, A.H., Stollenwerk, K.G. (Eds.), Arsenic in Ground Water, Geochemistry and Occurrence. Kluwer Academic Publishers, Boston, pp. 281–294.
- Langmuir, D., 1997. Aqueous Environmental Geochemistry. Prentice Hall, New York 600 p.
- Langmuir, D., Mahoney, J., Rowson, J., 2006. Solubility products of amorphous ferric arsenate and crystalline scorodite (FeAsO₄:2H₂O) and their application to arsenic behavior in buried mine tailings. Geochem. Cosmochim. Acta 70, 2942–2956.
- Langner, P., Mikutta, C., Kretzschmar, R., 2012. Arsenic sequestration by organic sulphur in peat. Nat. Geosci. 5, 66–73.
- Langner, P., Mikutta, C., Suess, E., Marcus, M.A., 2013. Spatial distribution and speciation of arsenic in peat studied with microfocused X-ray fluorescence spectrometry and Xray absorption spectroscopy. Environ. Sci. Technol. 47, 9706–9714.
- Lee, M.-K., Saunders, J.A., 2003. Effects of pH on metals precipitation and sorption: field bioremediation and geochemical modeling approaches. Vadose Zone J. 2, 177–185.
- Lee, M.-K., Saunders, J.A., Wilson, T., Levitt, E., Ghandehari, S.S., Dhakal, P., Redwine, J., Marks, J., Billor, M.Z., Miller, B., Han, D., and Wang, L. Field-scale bioremediation of arsenic-contaminated groundwater using sulfate-reducing bacteria and biogenic pyrite. Bioremed. J. (accepted).
- Le Pape, P., Blanchard, M., Brest, J., Jean-Claude Boulliard, J.-C., Ikogou, M., Stetten, L., Wang, S., Landrot, G., Morin, G., 2017. Arsenic incorporation in pyrite at ambient temperature at both tetrahedral S⁻¹ and octahedral Fe^{II} sites: evidence from EXAFS – DFT analysis. Environ. Sci. Technol. 51, 150–158.
- Lowers, H.A., Breit, G.N., Foster, A.L., Whitney, J., Yount, J., Uddin, M.N., Muneem, A.A., 2007. Arsenic incorporation into authigenic pyrite, Bengal Basin sediment. Bangladesh. Geochim. Cosmochim. Ac 71, 2699–2717.
- McArthur, J.M., Banerjee, D.M., Hudson-Edwards, K.A., Mishra, R., Purohit, R., Raverscroft, P., Cronin, A., Howarth, R.J., Chatterjee, A., Talukder, T., 2004. Natural organic matter in sedimentary basins and its relation to arsenic in anoxic groundwater: the example of West Bengal and its worldwide implications. Appl. Geochem. 9, 1255–1293.
- Mango, H., Ryan, P., 2015. Source of arsenic-bearing pyrite in southwestern Vermont, USA: sulfur isotope evidence. Sci. Total Environ. 505, 1331–1339.
- Neumann, T., Scholz, F., Kramar, U., Ostermaier, M., Rausch, N., Berner, Z., 2013. Arsenic in framboidal pyrite from recent sediments of a shallow water lagoon of the Baltic Sea. Sedimentology 60, 1389–1404.
- Nickson, R.T., McArthur, J.M., Ravenscroft, P., Burgess, W.S., Ahmed, K.M., 2000. Mechanism of arsenic poisoning of groundwater in Bangladesh and West Bengal. Appl. Geochem. 15, 403–413.
- Nickson, R., McArthur, J.M., Shrestha, B., Kyaw-Myint, T.O., Lowry, D., 2005. Arsenic and other drinking water quality issues, Muzaffargarh District. Pakistan. Appl. Geochem 20, 55–68.
- Nordstrom, D.K., Archer, D.G., 2003. In: Welch, A.H., Stollenwerk, K.G. (Eds.), Arsenic Thermodynamic Data and Environmental Geochemistry. In Arsenic in Ground Water: Geochemistry and Occurrence. Kluwer Academic Publishers, pp. 1–25.
- O'Day, P.A., Vlassopoulos, D., Root, R., Rivera, N., 2004. The influence of sulfur and iron on dissolved arsenic concentrations in the shallow subsurface under changing redox conditions. Proc. Natl. Acad. Sci. Unit. States Am. 101, 13703–13708.
- Ohmoto, H., Goldhaber, M.B., 1997. Sulfur and carbon isotopes. In: Barnes, H.L. (Ed.), Geochemistry of Hydrothermal Ore Deposits, third ed. John Wiley & Sons, NY, pp. 518–1613.
- Omoregie, E.O., Couture, R.-M., Van Cappellen, P., Corkhill, C.L., Charnock, J.M., Polya, D.A., Vaughan, D., Vanbroekhoven, K., Lloyd, J.R., 2013. Arsenic bioremediation by biogenic iron oxides and sulfides. Appl. Environ. Microbiol. 79, 4325–4335.
- Onstott, T.C., Chan, E., Polizzotto, M.L., Lanzon, J., DeFlaun, M.F., 2011. Precipitation of arsenic under sulfate reducing conditions and subsequent leaching under aerobic conditions. Appl. Geochem. 26, 269–285.
- Pi, K., Wang, Y., Xie, X., Ma, T., Su, C., Liu, Y., 2016. Role of sulfur redox cycling on arsenic mobilization in aquifers of Datong Basin, northern China. Appl. Geochem. 71, 31–43.
- Pi, K., Wang, Y., Xie, X., Ma, T., Liu, Y., Su, C., Zhu, Y., Wang, Z., 2017. Remediation of arsenic-contaminated groundwater by in-situ stimulating biogenic precipitation of iron sulfides. Water Res. 109, 337–346.
- Price, R.E., Pichler, T., 2006. Abundance and mineralogical association of arsenic in the Suwannee Limestone (Florida): implications for arsenic release during water–rock interaction. Chem. Geol. 228, 44–56.
- Qiu, G., Tianyu, G., Hong, J., Tan, W., Liu, F., Zheng, L., 2017. Mechanisms of arsenic containing pyrite oxidation by aqueous arsenate under anoxic conditions. Geochem. Cosmochim. Acta 217, 306–319.
- Reich, M., Kesler, S.E., Utsunomiya, S., Palenik, C.S., Chryssoulis, S.L., Ewing, R.C., 2005. Solubility of gold in arsenian pyrite. Geochem. Cosmochim. Acta 69, 2781–2796.
- Rickard, D.T., Luther III, G.W., 1997. Kinetics of pyrite formation by the H₂S oxidation of

- iron(II) monosulfide in aqueous solutions between 25°C and 125°C: the mechanism. Geochim. Cosmochim. Acta 61, 135–147.
- Rickard, D., Luther, G.W., 2007. Chemistry of iron sulfides. Chem. Rev. 107, 514–562.
 Rieder, M., Crelling, J.C., Šustai, O., Drábek, M., Weiss, Z., Klementová, M., 2007. Arsenic in iron disulfides in a brown coal from the north Bohemian basin, Czech Republic. Intl. J. Coal Geol. 71, 115–121.
- Rittle, K.A., Drever, J.I., Coldberg, P.J.S., 1995. Precipitation of arsenic during bacterial sulfate reduction. Geomicrobiol. J. 13, 1–11.
- Saunders, J.A., Swann, C.T., 1994. Mineralogy and geochemistry of cap rock Zn-Pb-Sr-Ba mineralization at Hazlehurst salt dome, Mississippi. Econ. Geol. 89, 381–390.
- Saunders, J.A., Cook, R.B., Thomas, R.C., Crowe, D.E., 1996. Coprecipitation of trace metals in biogenic pyrite: implications for enhanced intrinsic bioremediation. In: Bottrell, S.H. (Ed.), Proceedings, Fourth International Symposium of the Geochemistry of the Earth's Surface, Ilkley, U.K, pp. 470–474.
- Saunders, J.A., Pritchett, M.A., Cook, R.B., 1997. Geochemistry of biogenic pyrite and ferromanganese stream coatings: a bacterial connection? Geomicrobiol. J. 14, 203–217
- Saunders, J.A., Lee, M.-K., Wolf, L.A., Morton, C.M., Feng, Y., Thomson, I., Park, S., 2005a. Geochemical, microbiological, and geophysical assessments of anaerobic immobilization of heavy metals. Ann. Finance 9, 33–48.
- Saunders, J.A., Mohammad, S., Korte, N.E., Lee, M.-K., Fayek, M., Castle, D., Barnett, M.O., 2005b. Groundwater geochemistry, microbiology, and mineralogy of two arsenic-bearing Holocene alluvial aquifers from the USA. In: In: O'Day, P.A., Vlassopoulos, D., Ming, X., Benning, L.G. (Eds.), Advances in Arsenic Research: Integration of Experimental and Observational Studies and Implications for Mitigation. Am. Chem. Soc. Symposium Series, vol. 915. pp. 191–205.
- Saunders, J.A., Lee, M.-K., Uddin, A., Mohammad, S., Wilkin, R.T., Fayek, M., Korte, N.E., 2005c. Natural arsenic contamination of Holocene alluvial aquifers by linked tectonic, weathering, and microbial processes. Geochem. Geophys. Geos 6https://doi. org/10.1029/2004GC000803. Q04006.
- Saunders, J.A., Lee, M.-K., Shamsudduha, M., Chawdry, T., Ahmed, K.M., 2008. Geochemistry and mineralogy of arsenic under anaerobic conditions. Appl. Geochem. 23, 3205–3214.
- Saunders, J.A., Hofstra, A.H., Goldfarb, R.J., Reed, M.H., 2014. Geochemistry of hydrothermal gold deposits. In: second ed. In: Holland, H.D., Turekian, K.K. (Eds.), Treatise of Geochemistry, vol. 13. Elsevier, Oxford, pp. 383–424.
- Savage, K.S., Tingle, T.N., O'Day, P.A., Waychunas, G.A., Bird, D.K., 2000. Arsenic speciation in pyrite and secondary weathering phases, Mother Lode gold district. Tuolumne County, California. Appl. Geochem. 15, 1219–1244.
- Schoonen, M.A.A., Barnes, H.L., 1991. Reactions Forming Pyrite and Marcasite from Solution: I. Nucleation of FeS2 below 100°C 55. pp. 1495–1504.

- Schoonen, M.A.A., 2004. Mechanisms of sedimentary pyrite formation. In: In: Amend, J.P., Edwards, K.J., Lyons, T.W. (Eds.), Sulfur Biogeochemistry - Past and Present. GSA Special Papers, vol. 379. pp. 117–134.
- Seal II, R.R., 2006. Sulfur isotope geochemistry of sulfide minerals. Rev. Mineral. Geochem. 61, 633–677.
- Simon, G., Huang, H., Penner-Hahn, J.E., Kesler, S.E., Kao, L.-S., 1999. Oxidation state of gold and arsenic in gold-bearing arsenian pyrite. Am. Mineral. 84, 1071–1079.
- Smedley, P.L., Kinniburgh, D.G., 2002. A review of the source, behavior and distribution of arsenic in natural waters. Appl. Geochem. 17, 517–568.
- Southam, G., Saunders, J.A., 2005. Geomicrobiology of ore deposits. Econ. Geol. 100, 1067–1084.
- Stuckey, J.W., Schaefer, M.V., Kocar, B.D., Dittmar, J., Pacheco, J.L., Benner, S.G., Fendorf, S., 2015. Peat formation concentrates arsenic within sediment deposits of the Mekong Delta. Geochem. Cosmochim. Acta 149, 190–205.
- Sun, J., Quicksall, A.N., Chillrud, S.N., Mailloux, B.J., Bostick, B.C., 2016. Arsenic mobilization from sediments in microcosms under sulfate reduction. Chemosphere 153, 254–261.
- Walker, S.R., Parsons, M.B., Jamieson, H.E., Lanzirotti, A., 2009. Arsenic mineralogy of near-surface tailings and soils: influences on arsenic mobility and bioaccessibility in the Nova Scotia gold mining districts. Can. Mineral. 47, 533–556.
- Webster, J.G., 1990. The solubility of As_2S_3 and speciation of as in dilute and sulphide-bearing fluids at 25 and 90°C. Geochem. Cosmochim. Acta 54 1009–1007.
- Wilkin, R.T., Barnes, H.L., 1996. Pyrite formation by reactions of iron monosulfides with dissolved inorganic and organic sulfur species. Geochem. Cosmochim. Acta 60, 4167–4179.
- Wilkin, R.T., Wallschlager, D., Ford, R.G., 2003. Speciation of arsenic in sulfidic waters. Geochem. Trans. 4, 1–7.
- Wolthers, M., Charlet, L., van der Linde, P.R., Rickard, D.T., 2005a. Arsenic mobility in the ambient sulfidic environment: sorption of arsenic(V) and arsenic(III) onto disordered mackinawite. Geochem. Cosmochim. Acta 69, 3483–3492.
- Wolthers, M., Butler, I.B., Rickard, D., Mason, P.R.D., 2005b. Arsenic incorporation into pyrite at ambient environmental conditions: a continuous-flow experiment. In: In: O'Day, P.A., Vlassopoulos, D., Ming, X., Benning, L.G. (Eds.), Advances in Arsenic Research: Integration of Experimental and Observational Studies and Implications for Mitigation. Am. Chem. Soc. Symposium Series, vol. 915. pp. 60–76.
- Wolthers, M., Butler, I.B., Rickard, D.T., 2007. Influence of arsenic on iron sulfide transformations. Chem. Geol. 236, 217–227.
- Xie, X., Liu, Y., Pi, K., Liu, C., Li, J., Duan, M., Wang, Y., 2016. In situ Fe-sulfide coating for arsenic removal under reducing conditions. J. Hydrol 534, 42–49.
- Zouboulis, A.I., Kydros, K.A., Matis, K.A., 1993. Arsenic (III and V) removal from solutions by pyrite fines. Separ. Sci. Technol. 28 2449–246.